Synthesis of self-regenerating NiAl-Al2O3 composite coatings

R. Troncy, G. Bonnet, F. Pedraza

Synthesis of self-regenerating NiAl-Al_2O_3 composite coatings

R. Troncy[1, a], G. Bonnet[1, b], F. Pedraza[1, c]

[1] LaSIE, La Rochelle Université, UMR CNRS 7356, Avenue Michel Crépeau, 17042 La Rochelle Cedex 1, France

[a]romain.troncy1@univ-lr.fr, [b]gbonnet@univ-lr.fr, [c]fpedraza@univ-lr.fr

Keywords: Coating, Aluminothermic reaction; NiAl-Al_2O_3; Microstructure; Self-regenerating coating

Abstract

The aluminothermic reactions involved either in the mixtures or the stack of NiO and Al powders were elucidated in a previous work [1]. The present work now investigates the formation of potential self-regenerating coatings using the aluminothermic reaction between nickel oxide and aluminum. The use of this exothermic reaction allows the simultaneous formation of both alumina and nickel aluminides. The coatings were obtained by first pre-oxidizing the nickel substrate, then spraying an aluminum slurry before applying an adequate heat treatment. The most promising self-regenerating coatings display a first composite layer, made of an intermetallic compound (Al_3Ni or NiAl) and alumina, and a second layer with a higher concentration of oxide. The first layer is expected to play the role of an Al reservoir coating and the second one that of a diffusion barrier to slow down the Al flux to maintain the Al reservoir in the coating. The effects of preoxidation time and of temperature on the resulting coating microstructures are discussed as a function of time.

Introduction

Aluminum diffusion coatings manufactured by CVD-related techniques have long and widely been used for the protection of turbine blades made of Ni-based superalloys exposed to oxidative and corrosive conditions [2,3]. Some recent studies focused on slurry aluminizing via aqueous routes due to their milder ecological impact and much lower cost. The oxidation resistance of the slurry aluminide coatings was similar the one observed with traditional ones [4,5]. Pedraza et al. described the mechanisms of formation of such aluminide coatings on pure Ni [6] and Galetz and collab. [7] revealed the high exothermicity associated during the reaction of molten Al and Ni, which allowed the impressively quick formation of the coatings on different Ni-based superalloys [7,8].

However, irrespective of the fabrication mode (CVD or slurry), the Al from the diffusion coatings is mostly lost by diffusion into the substrate and diluted by the upward flow of the alloying elements upon exposure to high temperatures [9]. As a result, the Al reservoir of the coatings is depleted in particular with high activity coatings because of the significant Al gradient between the coating and the substrate [5]. While different approaches to slow down the Al inward diffusion have been proposed in the open literature, they all rely on placing diffusion barriers between the coating and the substrate mostly by using CVD [10], PVD [11], electrodeposition [12-14], and even by explosive welding, forming and heat treatment [15]. Such diffusion barriers can result in different coating compositions, microstructures and thicknesses that can be tailored as a function of the final application. Yet, none of these studies investigated the simultaneous formation of a hybrid coating like the ones derived from the well-known aluminothermic exothermic reactions that result in composite coatings made of nickel aluminides and alumina. For instance, Padmavardhani et al. sintered functionally graded NiAl-Al_2O_3 composite compounds by reactive hot compaction of powders [16]. Hot-pressing of pre-oxidized NiAl powder was

also employed to form NiAl-Al_2O_3 bulk samples with adequate bending strength and toughness [17]. One of our previous works highlighted the different reactive processes when mixing pre-oxidized Ni and metal Al vs. stacking metal Al onto pre-oxidized Ni. It was concluded that the particle size and preoxidation time governed the growth of the multilayered bulk samples made of nickel aluminides of different stoichiometries with various dispersions of the Al_2O_3 issued from the aluminothermic reaction [1]. Therefore, the goal of this paper is to extrapolate our previous findings to bulk samples to form potential self-regenerating coatings. The idea is to exploit the in situ exothermicity (with no external compaction) between the powders deposited from water-based slurries onto a pure Ni substrate to sinter the composite Ni_xAl_y-Al_2O_3 coatings. In addition, the high heat released during the aluminothermic reaction will be absorbed by the high thickness of the nickel, which will avoid the emission of gas or the projection of molten metal, as the work of K. Woll et al. as shown [18]. The mechanisms of formation of these original coatings are discussed for the first time in the literature.

1. Experimental procedure

Bulk Ni samples (99.98 wt. %, Goodfellow) were cut from 12.7 mm diameter cylindrical rods into coupons of about 1.5 mm thickness, polished with SiC P180 papers and then rinsed with deionized water and cleaned in ethanol before pre-oxidation at 1100°C for 2 h in air. After this pre-oxidation step, an Al-based slurry was sprayed on the coupons. The slurry formulation is based on a 1/10 PolyVinyl Alcohol (PVA)/deionized water solution to which 45 wt. % of spherical Al powders (4±3 µm, Hermillon Poudres, France) were added [12]. After blending, the slurries were deposited by airbrush on the pre-oxidized coupon samples. After each deposit, the samples were systematically dried in a stove at 50 °C for 30 min. The samples were weighed before and after slurry deposition with a 10^{-4}g precision balance to control the deposited slurry quantity.

The dry coatings were then annealed in a TGA apparatus to form the diffusion coating, under a flow of argon (20 mL/min) to prevent any significant oxidation of the substrate and of the Al particles [7]. The heat treatment was adapted to consider the thermal events observed in the differential scanning calorimetry (DSC, SETARAM Labsys Evo 1600) measurements [1]. This gave us three steps: at 620°C for 2 h to foster the solid/solid reduction between Al and NiO; 700°C for 2h to promote the liquid/solid aluminothermic reduction and the Al inward diffusion and a final step at 1080°C to terminate the aluminothermic reduction and foster the outward diffusion of Ni [6].

Two series of short (2 h) and long (12 and 24 h) heat treatment times were investigated (Fig. 1). In all of them, the heating and cooling rates were set at 5°C/min. In the short annealing series (Fig. 1a), temperature increments from 620 to 700 and finally to 1080°C were also investigated. In the long annealing series (Fig. 1b), the same temperatures were employed but the dwell times were longer (24h at 620 and at 700 °C and 12 h at 1080 °C). In the following, each heat treatment will be named through the last applied stage, for example: 620°C/2 h, 700°C/2 h or 1080°C/2 h, or 620°C/24 h.

Following these six different tests, the most promising heat treatments (700°C/24 h and 1080°C/2 h) were performed on the nickel substrate pre-oxidized for different times (30 min, 1 h, 1.5 h, 2 h), with a fixed quantity of deposited slurry (10±2 mg/cm²) to examine the influence of the effects of the nickel oxide layer.

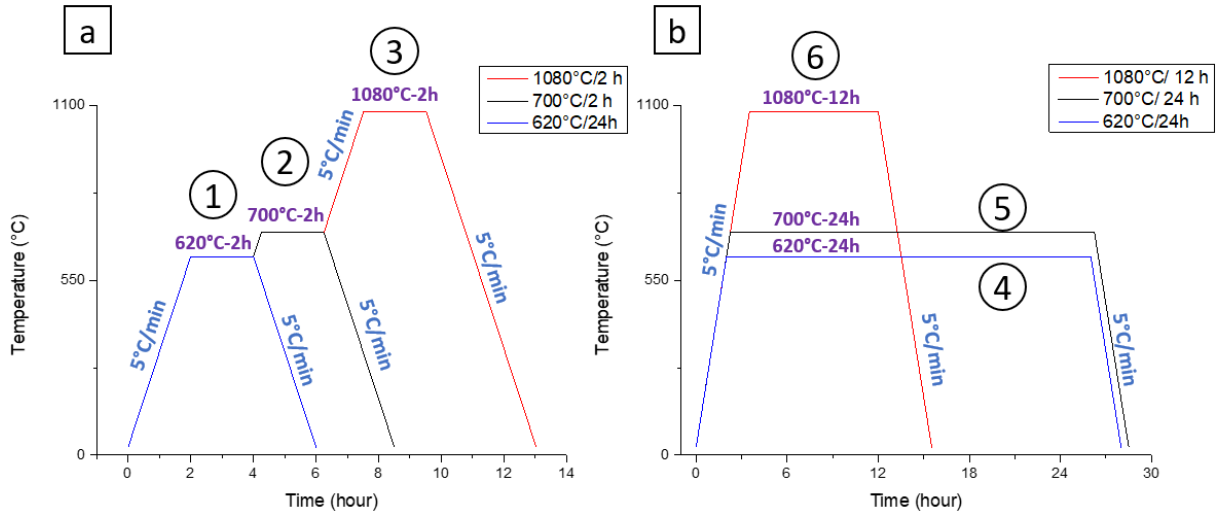

Fig. 1: Schematic drawing of the annealing treatments (a) short (dwell of 2h) and (b) long (dwells of 12 and 24 h) times of treatment.

The analyses and observations were done with a SEM (FEI QUANTA 200F) coupled to an EDAX detector for chemical analysis, at 20 kV under low vacuum (0.9 mbar). Raman micro-spectrometry (Jobin Yvon LabRam HR800, λ=632.82 nm) was also carried out to identify the different oxide phases. In addition, the crystal structure was characterized by X-ray diffraction (XRD) in a Bruker AXS D8 Advance with Cu $k_{\alpha 1}$ radiation (λ=0.15406 nm). The cross-sections were polished down to 1 µm water-based diamond suspension (Struers).

In addition, the SEM surface images of the pre-oxidized samples were processed with Photoshop to remove the oxide ridges. This step was required to reduce noise in the Image J treatment for the calculation of the areas and grain sizes of the oxides.

2. Results

2.1 Pre-oxidation of bulk Ni

The Ni substrates were pre-oxidized for 30 min, 1, 1.5 and 2 h at 1100 °C in air. The SEM micrographs taken on the surface and in the cross-section are shown in Fig. 2 in the secondary electron (SE) and backscattered electron (BSE) modes. The main results retrieved from image analysis are summarized in Table 1. Two morphologies of NiO (ridge-like and compact grains) can be observed at the surface of the samples for pre-oxidation times shorter than 1.5 h. For low temperature oxidation, the nickel oxides exhibit a cellular or platelet morphology. As the temperature increases, the morphology of the nickel oxide layer becomes ridge-like. In the literature [19-22], two mechanisms have been proposed to explain the formation of this morphology in the nickel oxide layers. One mechanism relates to the increased growth above grain boundary regions as a consequence of the rapid outward grain boundaries diffusion. Another suggested mechanism is that the ridges form at grain boundaries due to strong internal stress generated by internal oxide formation [19]. The oxide then releases by plastic deformation compressing the oxide and forming ridges. In addition, the amount of ridges would decrease with increasing oxidation time which in turn increases the thickness of the nickel oxide layer Fig. 2 and Table 1. Thicker oxide layers

decrease the cation outward diffusion, while the surface diffusion would remain constant and disperse the nickel oxide on the surface. Overall, the surface roughness is reduced. In our case, the amount of ridges decreases with increasing the pre-oxidation time (Table 1). Increasing the pre-oxidation times allows the oxide to expand from the grain boundaries towards the grain surface, which thus lowers the outward cation diffusion and decreases the growth stresses. In a similar vein, the size of the compact oxide grains increases with the exposure time (Fig. 3). Their growth is well reported in the literature to occur by outward lattice diffusion of Ni via singly or doubly charged Ni vacancies that leads to the columnar morphology [22] also observed in our study

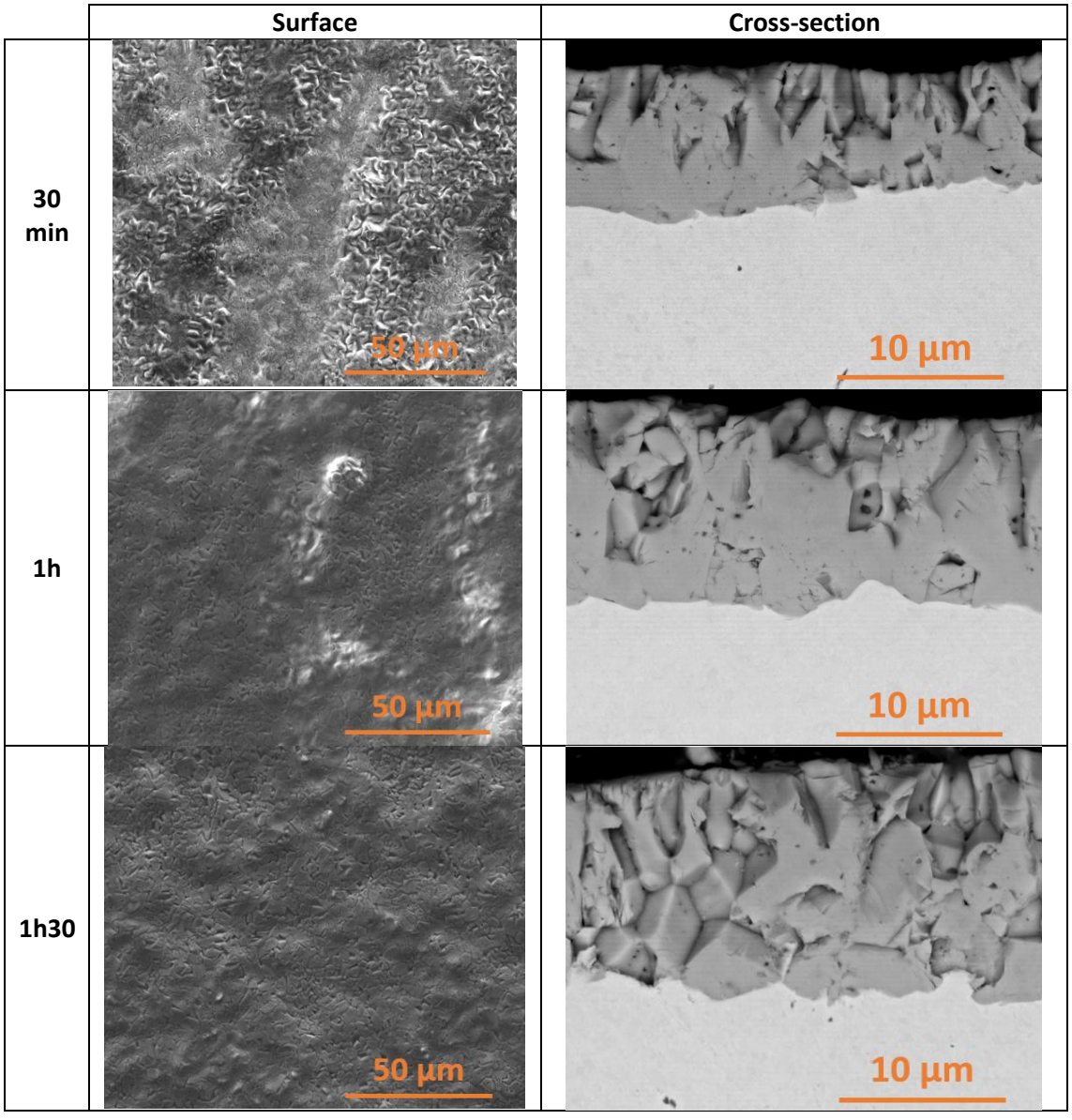

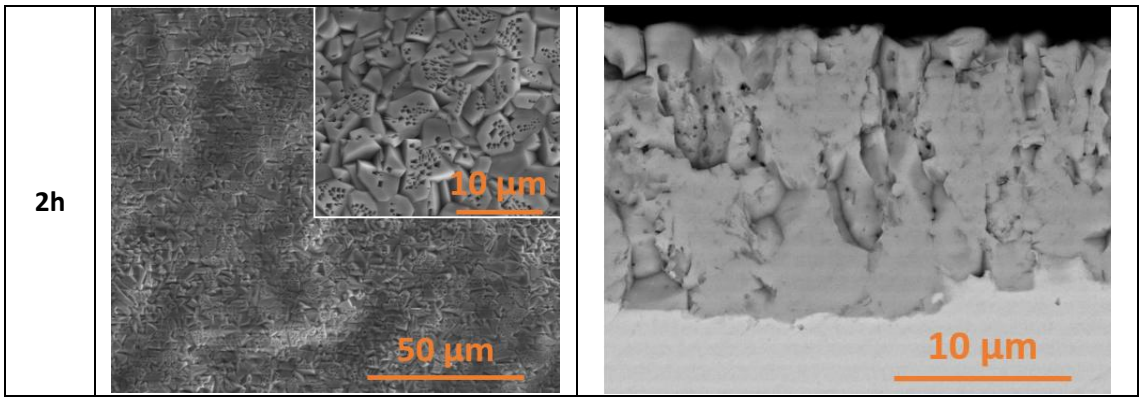

Fig. 2: SEM (SE and BSE mode) of surface and cross-section images on Ni samples pre-oxidized at 1100 °C under air for 30 min, 1, 1.5 and 2 h.

Table 1: Summary table of the ratio, thickness and size of the grains for different times of pre-oxidation.

Time	Compact grain area ratio (%)	Size of the compact grains (µm)	Thickness of the oxide layer (µm)
30 min	40.6	2±1	8±1.1
1h	72.8	2±1	12±1
1.5h	100	2±1	14±2
2h	100	3±1	15±2

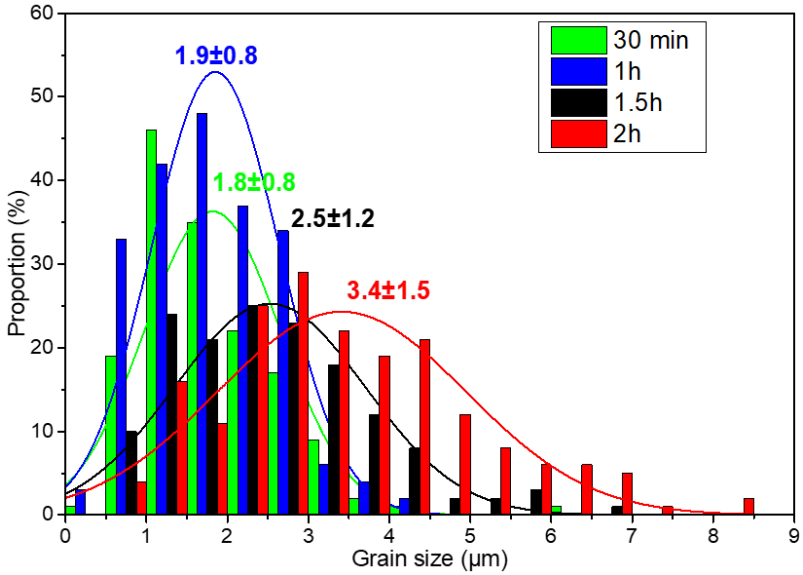

Fig. 3: Size and dispersion of the NiO compact grain sizes for the different pre-oxidation times at 1100 °C.

The 10 mg/cm² slurries deposited on the pre-oxidized samples are shown in Figure 4. The top layer of is 55±4 µm thick and contains the bright Al microparticles. (label 1 on Fig. 4). Below, the nickel oxide layer formed by oxidation at 1100 °C for 2 hours of the underlying nickel substrate is observed (label 2 on Fig. 4).

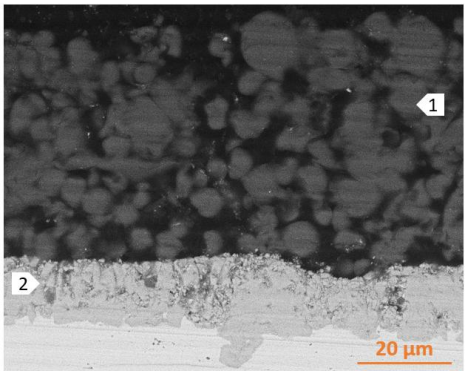

Fig. 4: Cross-section of the sample after application of the slurry on the pre-oxidized Ni substrate (1100 °C for 2 h).

2.2: Influence of the annealing temperature

The microstructures of the pre-oxidized (2 h) bulk Ni samples after reaction with Al at 620, 700 and 1080°C for 2 and 24 h are shown in Fig. 5. The compositions of the metallic elements in the observed layers are also given. The compounds formed and the thicknesses of the different layers are summarized in Table 2. They have been assessed by XRD, EDS and the Raman spectroscopy (Fig. 6).

Heat treatment at 620°C for 2 h and 24 h

After 2 h at 620°C (Fig. 5.a), only the outermost layer of NiO has reacted with Al to result in a porous Ni-rich layer of about 2.0±0.9 µm that also contains some oxide inclusions (Fig. 5.a, layer 1). The layer below corresponds to the part of NiO that did not react during the heat treatment (Fig. 5.a, layer 2). Indeed, the EDS analyses indicate that very little aluminum has diffused into this layer (Al-Ni 1-99 at. %). Increasing the time to 24 h results in a similar microstructure than after 2 h but now Al has diffused markedly (Fig. 5.b).

Heat treatment at 700°C for 2 h and 24h

The additional treatment at 700°C for 2 h brings about significant changes of the layers and of the microstructure (Fig.5.c). Indeed, a large part of the reduced Ni layer has reacted with Al to form an Al_3Ni intermetallic compound (Fig. 5.c, layer 1). However, a thin layer of metallic Ni still remains below the Al_3Ni layer (Fig. 5.c, layer 2). Then, the layer of NiO and the substrate are observed (Fig 5.c, layer 3). As opposed to 620°C/2h, a significant amount of Al has now diffused all across the layer of NiO (13 at. % Al) towards the substrate (9 at. % Al).

By increasing the reaction time to 24 h (Fig. 5.d), three layers can be distinguished over the substrate. The thickest (16±3 µm) most external layer is composed of an intermetallic/oxide composite, with an Al_3Ni intermetallic matrix and Al oxide shells surrounding the original Al particles (3.8±1.5 µm) (Fig. 5.d, layer 1). The central layer (thickness 8.7±1.8 µm) is composed of a cluster of oxides (Fig. 5.d, layer 2). This layer is separated from a 7.5±1.7 µm layer of unreacted NiO by a very thin layer of metallic Ni (Fig. 5.d, layers 3 and 4). In addition, the EDS analyses indicate that a significant Al has diffused through NiO to the substrate, with Al amounts of 23 and 16 at. % respectively.

Heat treatment at 1080°C for 2 and 12h

With the additional last heat treatments at 1080°C, the morphologies of the coatings are dramatically different from what was observed at lower temperatures. After 2 h, the first layer consists of NiAl intermetallic compound with Al_2O_3 inclusions (Fig. 5.e, layer 1) and surmounts a thin and compact layer of Al_2O_3 (Fig. 5.e, layer 2). Then, the fine layer of Ni appears above the layer of NiO and the substrate (Fig. 5.e, layers 3 and 4). Finally, the pattern of the NiAl grains of the first layer (Fig.5.e layer 1) seems to be close to those observed for the nickel oxide layer (Fig.5.e layer 4).

After 12 h, the coating is mainly composed of NiAl but three inhomogeneous sub-layers can be observed (Fig. 5.f). The first sub-layer is characterized by the presence of numerous pores (Fig. 5.f, layer 1). The second one is quite similar to the one observed after 24 h at 620 and 700 °C, with the presence of Al_2O_3 clusters (Fig. 5.f, layer 2). The third layer is very uneven and contains large oxidized cavities extending into the 4th layer that is composed of NiAl (Fig. 5.f, layer 4). One can also note the delamination between the coating and the substrate probably due to a difference of their thermal expansion coefficients.

	Spot	Al (at %)	Ni (at%)
620°C/2 h			
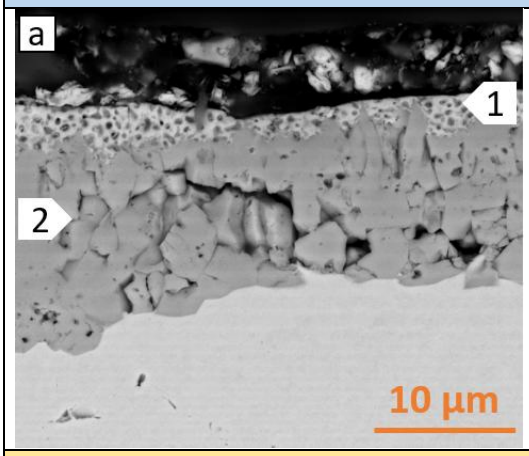	**1**	1	99
	2	42	58
620°C/24 h			
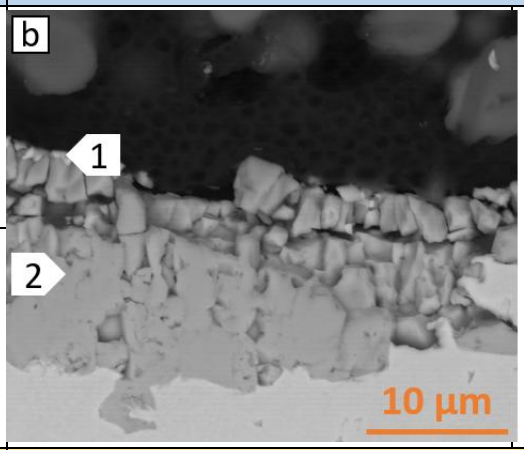	**1**	39	61
	2	14	86
700°C/2 h			
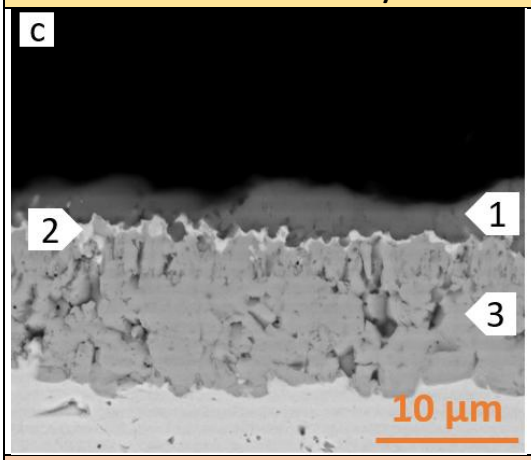	**1**	67	33
	2	17	83
	3	13	87
700°C/24 h			
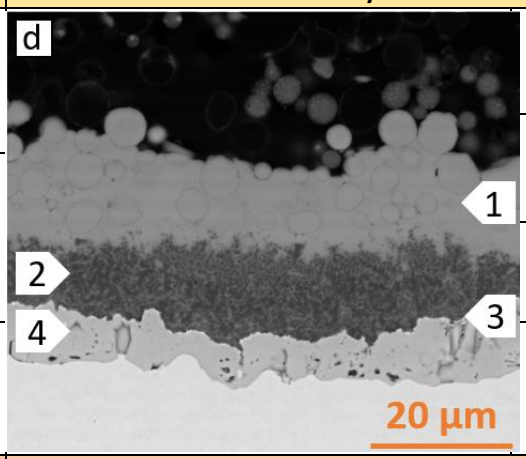	**1**	76	24
	2	84	16
	3	44	56
	4	23	77
1080°C/2 h			
1080°C/12 h			

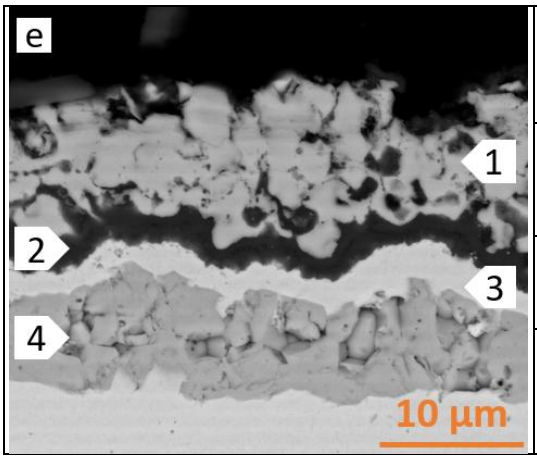

1	43	57
2	81	19
3	9	91
4	8	92

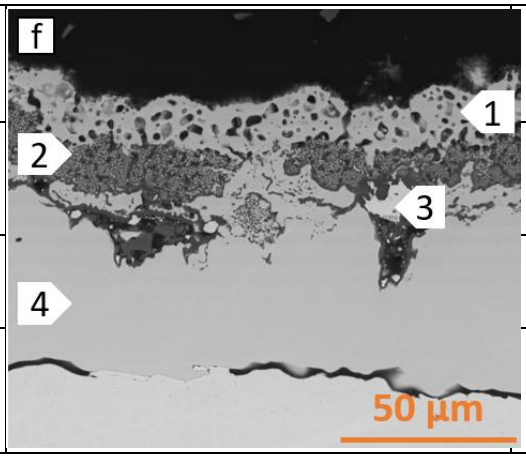

1	52	48
2	75	25
3	20	80
4	44	56

Fig. 5: SEM (BSE mode) cross-sections of the samples pre-oxidized at 2h for 1100°C and subsequent annealing of the Al-slurry coating at 620°C (a and b), 700°C (c and d) and 1080°C (e and f) for 2, 12 or 24 h.

Table 2: Summary table of the different compounds and thicknesses of the samples after the heat treatment.

Figure			**6.a**				**6.b**	
Layer	1	2	3	4	1	2	3	4
Compounds	Ni + pores	NiO	Substrate	---	Ni	NiO	Substrate	---
Thickness (µm)	2.9±1	1.8±1.8	---	---	1±0.2	13.2±1.8	---	---
Figure			**6.c**			**6.d**		
Compounds	Al_3Ni	Ni	NiO	Substrate	Al_3Ni	Cluster of Al_2O_3	Ni	NiO
Thickness (µm)	3.1±0.9	0.6±0.5	10.2±0.6	---	15.5±3	8.7±2	0.2±0.1	7.5±2
Figure			**6.e**			**6.f**		
Compounds	NiAl + α-Al_2O_3	α-Al_2O_3	Ni	NiO	NiAl + pores	Cluster of α-Al_2O_3	Oxidized cavities	NiAl
Thickness (µm)	9.8±1.5	2.4±0.6	2.4±0.7	6.9±0.7	14.4±2	12.3±4	8.1±6	52.7±4

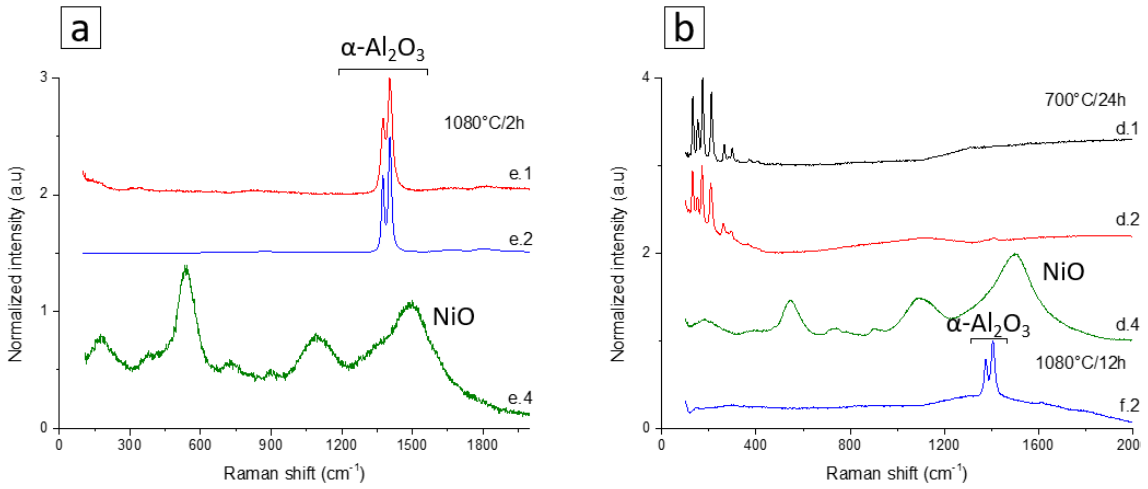

Fig. 6: Raman spectra on the cross-sections of 2 h pre-oxidized samples after the heat treatments 1080°C/2h (a), 700°C/24 h and 1080°C/12 h (b).

2.3 Influence of the pre-oxidation time of the nickel substrate

Following the results presented in section 2.2, the most promising heat treatments for a possible self-regenerating coating application appear to be 1080°C/2 h and 700°C/24 h. Therefore, the study of the influence of the pre-oxidation of the nickel substrate was exclusively conducted with such heat treatments. The pre-oxidation times were thus set at 30 min, 1 h and 1.5 h. The microstructures and metal contents in the coatings after the heat treatments are given in Fig. 7. Table 3 summarizes the crystallographic compounds assessed by XRD, EDS and Raman spectroscopy (Fig. 8), and the thicknesses of the different layers (from SEM images).

	1080°C/2 h	Spot	Al (at %)	Ni (at%)	700°C/24 h	Spot	Al (at %)	Ni (at%)
30 min	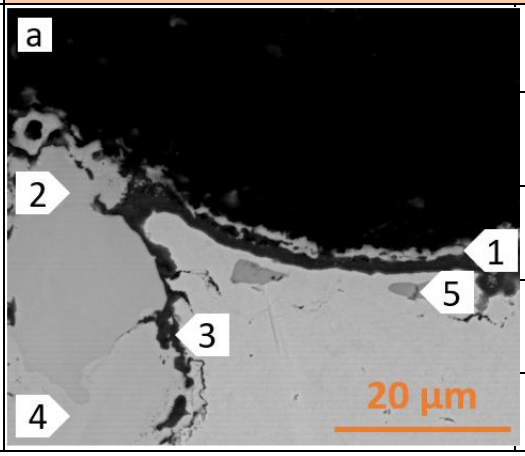	1	45	55	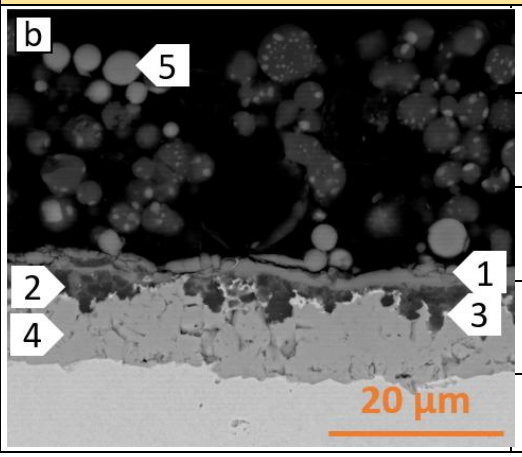	1	74	26
		2	35	65		2	82	18
		3	63	37		3	28	72
		4	24	76		4	17	83
		5	9	91		5	76	24

1h	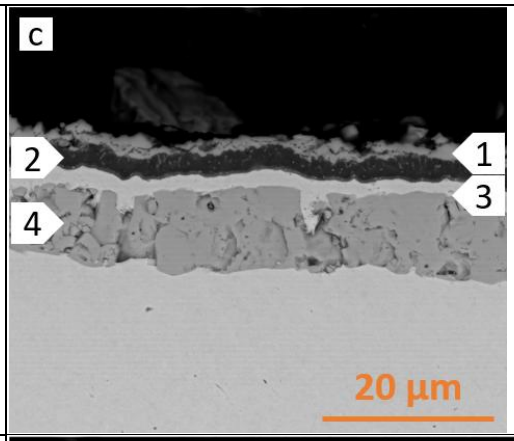	**1**	59	41	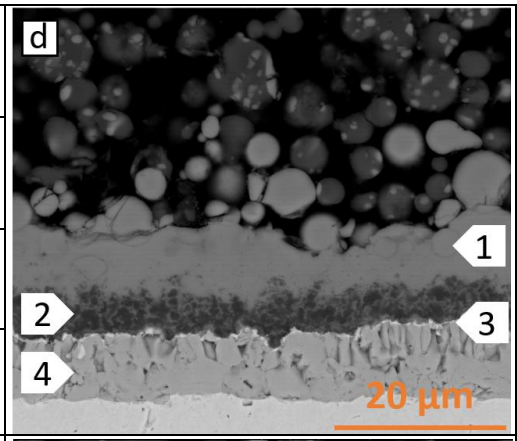	**1**	77	23
		2	84	16		**2**	85	15
		3	10	90		**3**	75	25
		4	6	94		**3**	11	89
1.5h	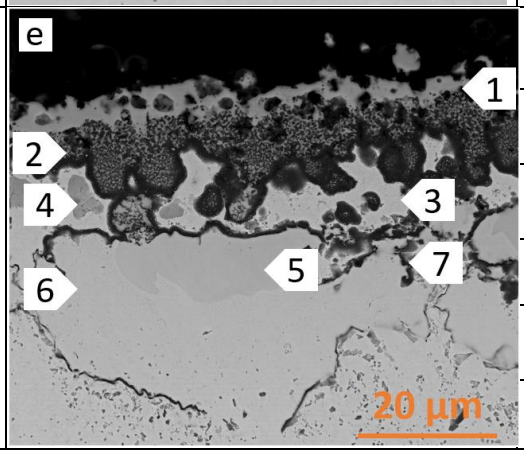	**1**	47	53	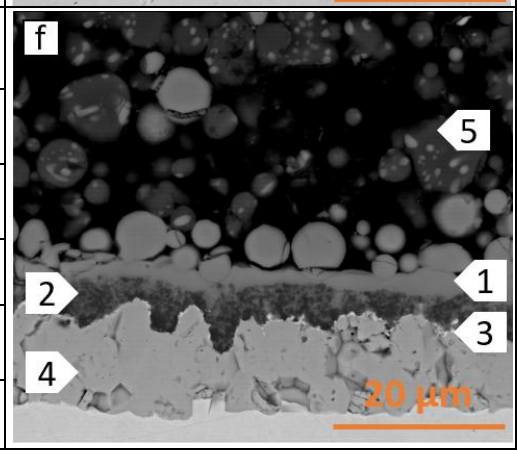	**4**	23	77
		2	70	30		**2**	79	21
		3	11	89		**3**	22	78
		4	10	90		**4**	15	85
		5	27	73		**5**	94	6
		6	15	85		**6**		

Fig. 7: SEM (BSE mode) cross-sections of the pre-oxidized samples at 30 min, 1 h and 1.5 h for 1100 °C after TGA treatment at 1080°C/2h and 700°C/24 h.

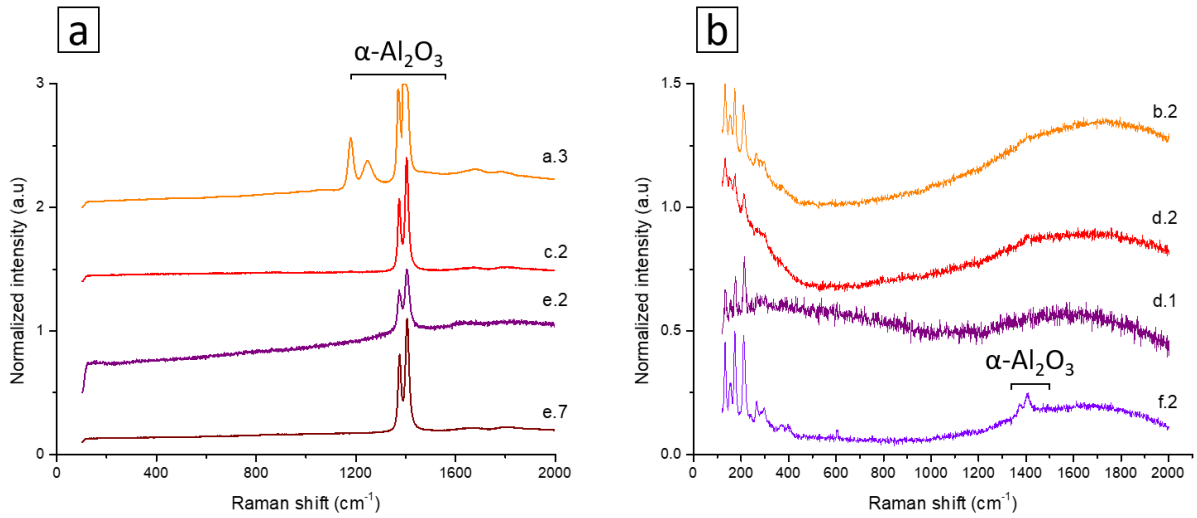

Fig. 8: Raman spectra on the cross-sections of samples pre-oxidized for 30 min, 1 and 1.5 h made after the heat treatments 1080°C/2 h (a) and 700°C/24 h (b).

2.3.1 Heat treatment of 1080°C/2h

For the heat treatment 1080°C/2 h applied on a Ni sample pre-oxidized for 30 min, the coating presents a non-homogeneous structure because the areas made of "diffusion islands" alternate with more homogeneous zones. The diffusion islands are composed of a NiAl (Fig. 7.a label 1) and Ni_3Al core (Fig. 7.a label 1) surrounded by aluminum oxide (Fig. 7.a label 3). The more homogeneous area is made up of a first layer of NiAl, embedding alumina particles that surmounts a thick layer of aluminum oxide, nickel and NiO. It can be noted that only a few discontinuous areas of NiO remain (Fig. 7.a label 5), i.e. most of the NiO has been consumed.

With 1 h of pre-oxidation, the diffusion islands can no longer be observed and the coating exhibits a more homogeneous aspect. Like with the 30 min of pre-oxidation, the first layer consists of an intermetallic compound (Fig. 7.c label 1) that surmounts an alumina layer (Fig. 7.c label 2) whose thickness is similar to the previous one. Finally, Ni resulting from NiO reduction (Fig. 7.c label 3) and the remaining NiO can be observed closer to the substrate (Fig. 7.c label 4).

For a pre-oxidation time of 1.5 h, the coating shows a very different structure, except for the first layer (Fig. 7.e label 1) (NiAl embedding alumina particles). Below, a composite structure comprising Al_2O_3 and NiAl is found whose thickness is uneven and delimited by a dense layer of alumina (Fig. 7.e label 2). Underneath, a Ni layer (Fig. 7.e label 3) with NiO islands (Fig. 7.e label 4) appears over the Ni substrate (Fig. 7.e label 6) containing aluminized areas (Fig. 7.e label 5) and alumina particles (Fig. 7.e label 7).

2.3.2 Heat treatment of 700°C/24h

For the heat treatment 700°C/24 h, the coatings appear rather similar to the one shown in Fig. 5.d (section 2.2) irrespective of the pre-oxidation time. Four different layers can again be observed. The top layer made of the intermetallic compound Al_3Ni (Fig. 7.b,d,f label 1) surmounts an aluminum oxide cluster (Fig. 7.b,d,f label 2), then a thin layer of Ni resulting from the NiO reduction (Fig. 7.b,d,f label 3) and finally, the remaining NiO (Fig. 7.b,d,f label 4). Their thicknesses and compositions are however somewhat different (see Table 3). In addition, the coating contains no trapped particles when the pre-oxidation is conducted for just 30 min (Fig. 7.b label 1).

Table 3: Summary table of the different compounds and thicknesses of the coating layers resulting from the heat treatments of the slurry after TGA treatment (1080°C/2 h and 700°C/24 h).

	1080°C/2 h				**700°C/24 h**			
Figure	**7.a**				**7.b**			
Layer	1	2	3	4	1	2	3	4
Compounds	NiAl	Al_2O_3	Ni	NiO	Al_3Ni	Cluster of Al_2O_3	Ni	NiO
Thickness (µm)	1.1±0.5	1.6±0.3	1±0.2	1.1±0.5	2.1±0.5	3±1.3	0.4±0.3	7.8±1.4
Figure	**7.c**				**7.d**			
Compounds	NiAl	Al_2O_3	Ni	NiO	Al_3Ni	Cluster of Al_2O_3	Ni	NiO
Thickness (µm)	1.7±0.7	2.6±0.3	1.7±0.3	9±0.8	5±1.5	2.4±1.2	0.4±0.3	9.5±1.8
Figure	**7.e**				**7.f**			
Compounds	NiAl	Cluster of Al_2O_3	Ni	NiO	Al_3Ni	Cluster of Al_2O_3	Ni	NiO
Thickness (µm)	3.4±1.3	9.6±3.4	2.3±3.5	2.8±1.8	3.7±1.9	3.9±1.4	0.3±0.2	10±2

3. Discussion

3.1: Influence of the heat treatment on the formation mechanisms of coatings

Concerning the heat treatment at 620°C, the observed phenomena are identical when the heat treatment is of 2 or 24 h and barely any aluminothermic reaction occurred. In contrast, significant differences appear when the temperature is raised to 1080°C (short times) or the times are extended (24 h) at intermediate temperature (700°C).

For the short times (2 h at 620 and at 700°C) till 1080°C/2 h, a sequence for the mechanisms of formation of the coatings is schematically depicted in Fig. 9. When the temperature reaches 517±15°C [1], an aluminothermic reaction between the Al microparticles and NiO starts at their interface (eq. 1). This solid/solid reaction of reduction results in the formation of a thin layer (2.9±1 µm) of metallic Ni after 2 h at 620°C (Fig. 9.a).

$$Al + NiO = Al_2O_3 + Ni \ (eq. 1)$$

Then, at a temperature of about 660°C, Al melts and begins to dissolve the Ni product near the interface and provokes a competition reaction between the formation and the dissolution of the eutectic Al_3Ni [7]. During this step, no aluminothermic reaction takes place [1,14].

When the temperature increases and approaches 700°C, the formation of the Al_3Ni intermetallic is assumed to be sufficiently fast (eq. 2) to overcome its dissolution (3 µm after 2 h (Fig. 9.b)).

$$Al_{(l)} + Ni = Al_3Ni \ (eq. 2)$$

At higher temperature (1080°C), the Ni content locally increases and causes the transformation of Al_3Ni into solid Al_3Ni_2 (eq. 3) and then into NiAl (eq. 4) (Fig. 9.c). The alumina formed during this step gets stuck at the grain boundaries of the NiO, depicting the pattern of nickel oxide shown in Fig. 5.e and 5.f.

$$Al_3Ni_{(l)} + Ni_{(l)} = Al_3Ni_{2(s)} \ (eq. 3)$$

$$Al_3Ni_{2(s)} + Ni_{(s)} = NiAl_{(s)} \ (eq. 4)$$

$$Al_{(l)} + NiO_{(s)} = Al_2O_3 + Ni \ (eq. 5)$$

One shall note that these reactions are assumed to be fostered by the local temperature increase related to the high exothermicity involved in the dissolution of Ni in molten Al [7,8]. Therefore, the alumina formed by aluminothermic reaction (eq. 5) rapidly segregates at the interface between the intermetallic and the NiO, further reducing matter exchange, which stops the aluminothermic reaction (Fig. 9.d). The combined thickening of alumina and the increased Ni content of the intermetallic lower the solid-state diffusion and the overall activity of the system [18,23-24].

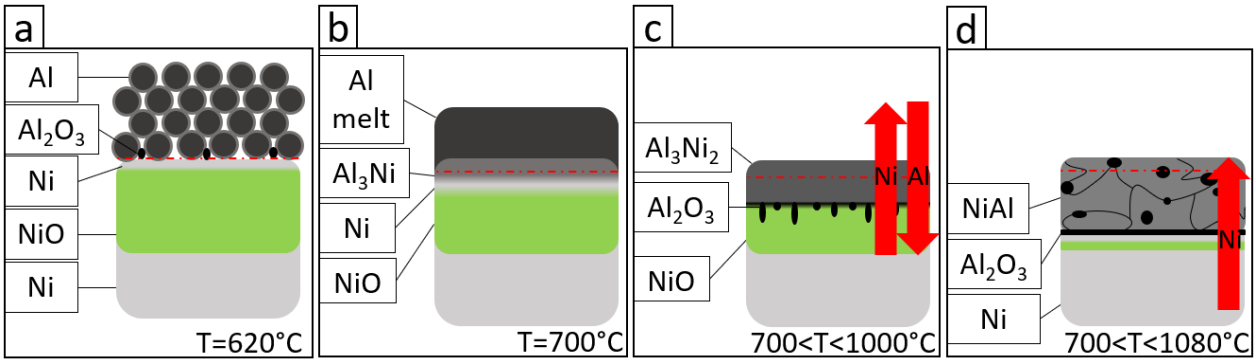

Fig. 9: Schematic drawing of the aluminothermic reduction and reaction between a pre-oxidized Ni substrate and Al particles heated by stages till 1080°C.

In contrast, the evolution of the coating is quite significant at 700°C/24 h (Fig. 10.a). Initially, the solid/solid aluminothermic reactions followed by melting of Al and the formation/dissolution of the eutectic Al_3Ni occur (Fig. 10.b). However, two different microstructures of the coatings have been observed.

A first microstructure (Figure 10.c) results from the aluminothermic reaction between molten Al and NiO (eq. 5). This reaction brings about the formation of Al_2O_3 that segregates at the Al/NiO interface. While compact, the alumina layer is relatively discontinuous and therefore restricts the diffusion phenomena between the species without blocking them fully. As a result, the thickness of alumina increases till a threshold value (~5 µm) over which interdiffusion is arrested and the remaining NiO cannot be reduced.

In the second coating microstructure (Fig. 10.d), the initial development is assumed to be quite similar. However, the Al_2O_3 grains issued from the aluminothermic reactions form clusters that do not slow down sufficiently direct contact of molten Al with the newly formed Al_3Ni. This exothermic reaction brings about the dissolution of the intermetallic component and the Al_2O_3 clusters to float over the melt. The subsequent aluminothermic reaction will keep on producing the Al_2O_3 clusters dispersed in the intermetallic layer. The end of the reactions can occur by either an insufficient amount of Al that would stop the aluminothermic reaction, but this does not seem to be the case, or by the increased amount of Al_2O_3 in the coating, which appears in line with the experimental observations because Al_2O_3 both blocks interdiffusion of the species and lowers the local temperature given the fact that Al_2O_3 is an inert heat absorber [24].

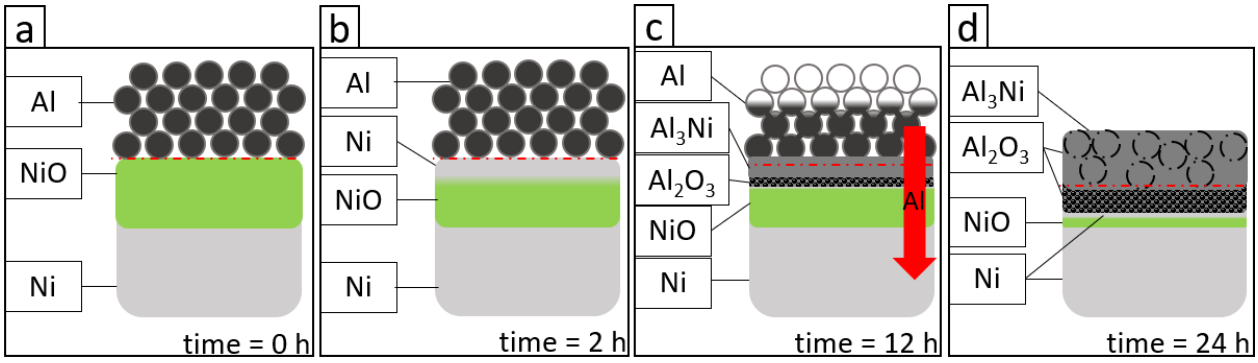

Fig. 10: Schematic drawing of the aluminothermic reduction and reactions between a preoxidized Ni substrate and Al particles heated at 700°C during 24 h

3.2: Influence of the pre-oxidation time

- 700°C/24 h

The coating microstructures obtained after 24 h at 700°C on the substrate pre-oxidized for different times do not differ markedly. In particular, the thin NiO scale formed after just 30 min of pre-oxidation remains almost identical (Fig. 11). In contrast, a greater permeability of Al through the NiO layer to form Al_3Ni is obtained with longer pre-oxidation times (Fig. 11.a). This can be interpreted on the basis of the vacancy concentration in the oxide. Indeed, NiO is a p-type semiconductor, which implies that thickening of the oxide takes place by outward cation diffusion hence leading to a porous scale (Fig. 12.a). In addition, different studies reported that the NiO oxide scale develop a continuous network of pores and cracks that reach the substrate [22,25-30] due to many different reasons including the dissociation of the oxide along the defects (grain boundaries, porosity, etc.) [31-34], cracking induced by the internal stresses [25,35-38] and opening of the microcracks related to different diffusion rates within the oxide scale (Fig. 12.b) [38]. In this study, we hypothesize that the molten Al and Al_3Ni can pass through these channels by capillarity. This is supported by the fact that the 1.5 h pre-oxidized nickel does not form homogeneous clusters of Al_2O_3 after annealing the coatings till 1080°C/2 h and 700°C/24 h (Fig. 12.c). In contrast, the Al_2O_3 seems to segregate at the channels and grain boundaries of NiO (Figs. 12.c). Furthermore, the Al-rich flux does not reach the Ni/NiO interface because (i) the defects in the oxide are too discontinuous to allow a regular flow of Al and/or diffusion of Ni to form the Al_3Ni, (ii) the Al activity lowers significantly, hence limiting the aluminothermic reaction and the interdiffusion of the species and (iii) the Al_2O_3 layer grows over the critical threshold and blocks the direct contact of Al with Ni. Very likely, a combination of the three phenomena occurs but (iii) appears more plausible and is coherent with the significant amounts of Al_2O_3 shown in the coatings and with the fact that Al particles get trapped by outward diffusion of Ni (Fig. 12.d).

- 1080°C/2 h

As opposed to 700°C/24 h, the pre-oxidation time exerts a great influence on the aluminothermic reaction and on the aluminizing of the nickel substrate. Indeed, for the samples pre-oxidized 30 min and 1 h, the Al_2O_3 resulting from the aluminothermic reaction blocks the reaction between Al and Ni. As a result, the reaction is stopped and the substrate cannot be aluminized. For longer pre-oxidation times (1.5 h), the Al_2O_3 mimics the shape of the former NiO grains. This suggests that molten Al and/or Al_3Ni permeates through the defects of NiO and that reduction of half of the NiO thickness has occurred (Fig. 11.b). Finally, for a preoxidation time of 2h, the dark contrast of layer 1 shown in the backscattered electron mode of Fig. 5.e corresponds to Al_2O_3 surrounding the grains of NiAl. Therefore, Raman spectra in these local areas and in the continuous layer 2 were conducted (Fig. 6). The α-Al_2O_3 polymorph is clearly inferred from the doublet in the fluorescence region. Atkinson and Taylor [39,40] demonstrated that the thickness of the grain boundaries is around 70 Å. It can be assumed that during the heat treatment, the aluminum oxide would segregate where there is vacant space.

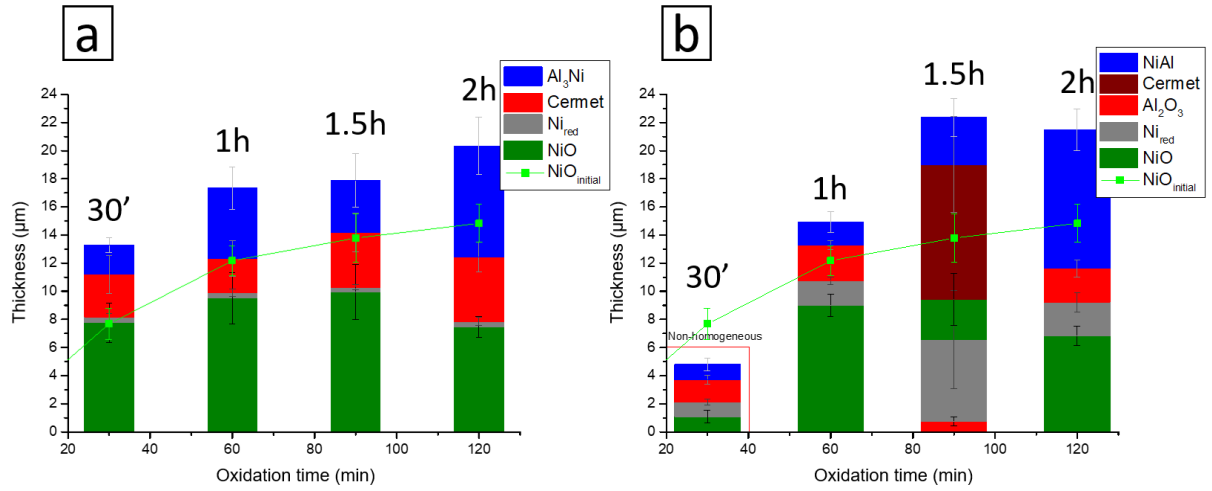

Fig. 11: Histogram of the thicknesses of the different formed layers for a heat treatment 700°C/24 h (a) and 1080°C/2 h (b) applied after different Ni substrate pre-oxidation times.

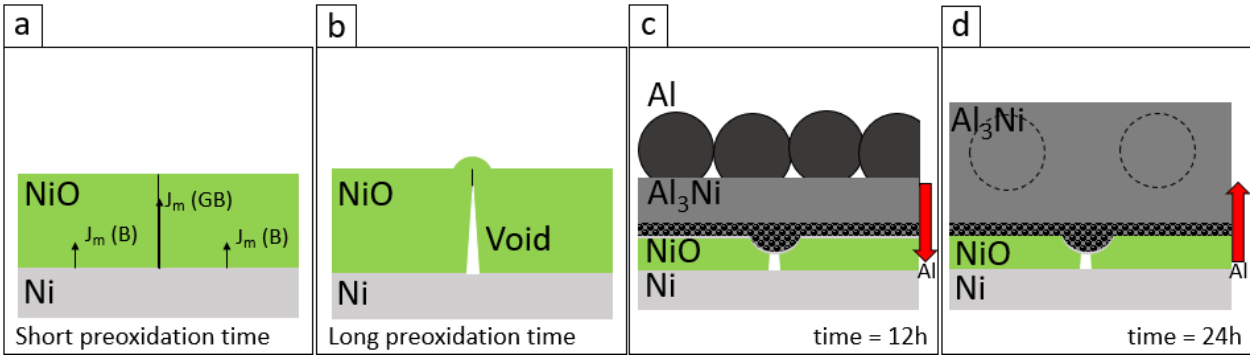

Fig. 12: Schematic drawing of the aluminothermic reduction and reactions between pre-oxidized Ni substrate and Al particles heated at 700°C during 24 h.

Conclusions

The formation of potential self-regenerating coatings with Al-rich Ni_xAl_y phases and Al_2O_3 dispersion has been investigated using aluminothermic reactions on pre-oxidized nickel substrate. It has been found that one key parameter to achieve even coatings is the duration of the preoxidation of the substrate. The short pre-oxidation times (< 1 h) grow a “ridge-like” morphology of NiO that impedes the homogeneous aluminization of the substrate. The longer pre-oxidation times (1<t<2 h) leads to the growth of compact grains that allows the aluminothermic reaction to occur, hence to obtain even aluminized layers. It is believed that the increase in the permeability of NiO to Al is due to the many defects present in the oxide layer caused by the major diffusion of Ni^{2+} cations to the oxide surface.

One of the promising coatings was sintered by pre-oxidizing the Ni substrate for 2 h followed by a slurry aluminizing at 700°C for 24 h. The coating consists of a first layer of Al_3Ni and alumina microspheres and a second layer with a composite microstructure between the alumina and the intermetallic compound. However, an unreacted NiO layer remained over the substrate even after 24 h of aluminizing. It thus appears that the control of the thickness of the NiO oxide needed for the reduction could be achieved by

electroplating nickel layers onto the substrates to be coated, which shall be investigated. Similarly, the interdiffusion behavior should be studied to assess the regenerating effect of the coatings $Al_3Ni + Al_2O_3$.

References

[1]: R. Troncy, G. Bonnet, F. Pedraza, Microstructural characterization of NiAl–Al_2O_3 composite materials obtained by in situ aluminothermic reduction of NiO for potential coating applications, Materials Chemistry and Physics 251 (2020) 123-124.

https://doi.org/10.1016/j.matchemphys.2020.123124

[2]: G.W. Goward, Current research on the surface protection of superalloys for gas turbine engines, JOM 22 (1970) 31-39.

https://doi.org/10.1007/BF03355665

[3]: J. Stringer, High-temperature corrosion of superalloys, Material Science and Technology 3(7) (1987) 482-493.

https://doi.org/10.1080/02670836.1987.11782259

[4]: B.G. Mc Mordie, Oxidation resistance of slurry aluminides on high temperature titanium alloys, Surface and Coating Technology 49 (1991) 18-23.

https://doi.org/10.1016/0257-8972(91)90025-R

[5]: B. Rannou, B. Bouchaud, J. Balmain, G. Bonnet, F. Pedraza, Comparative isothermal oxidation behavior of new aluminide coatings from slurries coating Al particles and conventional out-of-pack aluminide coatings, Oxidation of Metals 81 (2014) 139-149.

https://doi.org/10.1007/s11085-013-9427-6

[6]: F. Pedraza, M. Mollard, B. Rannou, J. Balmain, B. Bouchaud, G. Bonnet, Potential thermal barrier coating systems from Al microparticles. Mechanisms of coating formation on pure nickel, Materials Chemistry and Physics 134 (2012) 700–705.

https://doi.org/10.1016/j.matchemphys.2012.03.053

[7]: M.C. Galetz, X. Montero, M. Mollard, M. Günthner, F. Pedraza, M. Schütze, The role of combustion synthesis in the formation of slurry aluminization, Intermetallics 44 (2014) 8–17.

https://doi.org/10.1016/j.intermet.2013.08.002

[8]: A. Biswas, S.K. Roy, K.R. Gurumurthy, N. Prabhu, S. Banerjee, A study of self-propagating high-temperature synthesis of NiAl in thermal explosion mode, Acta Materialia 50 (2002) 757-773.

https://doi.org/10.1016/S1359-6454(01)00387-1

[9]: E. Perez, T. Patterson, Y. Sohn, Interdiffusion analysis for NiAl versus superalloys diffusion couples, Journal Phase Equilibria and Diffusion, 27(6) (2006) 659-664.

https://doi.org/10.1007/bf02736569

[10]: J. Müller, M. Schierling, E. Zimmermann, D. Neuscütz, Chemical vapor deposition of smooth α-Al_2O_3 films on nickel base superalloys as diffusion barriers, Surface and Coatings Technology 120-121 (1999) 16-21.

https://doi.org/10.1016/S0257-8972(99)00333-3

[11]: C. Guo, W. Wang, Y. Cheng, S. Zhu, F. Wang, Yttria partially stabilized zirconia as diffusion barrier between NiCrAlY and Ni-base single crystal René N5 superalloy, Corrosion Science 94 (2015) 122-128.

https://doi.org/10.1016/j.corsci.2015.01.048

[12]: B. Bouchaud, B. Rannou, F. Pedraza, Slurry aluminizing mechanisms of Ni-based superalloys incorporating an electrosynthesized ceria diffusion barrier, Materials Chemistry and Physics 143 (2013) 416-424.

https://doi.org/10.1016/j.matchemphys.2013.09.022

[13]: H. Liu, M.M. Xu, S. Li, Z.B. Bao, S.L. Zhu, F.H. Wang, Improving cyclic oxidation resistance of Ni_3Al-based single crystal superalloy with low-diffusion platinum-modified aluminide coating, Journal of Materials Science & Technology 54 (2020) 132-143.

https://doi.org/10.1016/j.jmst.2020.05.007

[14]: Y.F. Yang, P. Ren, Z.B. Bao, S.L. Zhu, F.H. Wang, W. Li, Microstructure and cyclic oxidation of a Hf-doped (Ni,Pt)Al coating for single-crystal superalloys, Journal Materials of Science 55 (2020) 11687-11700.

https://doi.org/10.1007/s10853-020-04782-5

[15]: V.G. Shmorgun, L.D. Iskhakova, A.I Bogdanov, A.O. Taube, Phase composition of heat-resistance layered coatings of the Al-Cr-Ni system, Metallurgist 60 (9-10) (2017) 1113-1119.

https://doi.org/10.1007/s11015-017-0414-z

[16]: D. Padmavardhani, A. Gomer, R. Abbaschian, Synthesis and microstructural characterization of NiAl-Al_2O_3 functionally gradient composites, Intermetallics 6 (1998) 229-241.

https://doi.org/10.1016/S0966-9795(97)00076-9

[17]: C.S. Hwang, T.J. Liu, Microstructure and mechanical properties of NiAl/Al_2O_3 composites, Journal of Materials research 14(01) (1999) 75-82.

https://doi.org/10.1557/JMR.1999.0013

[18]: K. Woll, J. David Gibbins, K. Slusarski, A.H. Kinsey, T.P. Weihs, The utilization of metal/metal oxide core shell-powders to enhance the reactivity of diluted thermite mixtures, Combustion and Flame 167 (2016) 259-267.

https://doi.org/10.1016/j.combustflame.2016.02.006

[19]: R. Peraldi, D. Monceau, B. Pieraggi, in: M. McNallan, E. Opila, T. Maruyama, T. Narita (Eds.), High

Temperature Corrosion and Materials Chemistry (Electrochem. Soc. Proc., vol. 99–38) , 1999, p. 204.

[20]: R. Peraldi, D. Monceau, B. Pieraggi, Correlations between growth kinetics and microstructure for scales formed by high-temperature oxidation of pure nickel, I. Morphologies and Microstructures, Oxidation of Metals 58 (2002) 249-273.

https://doi.org/10.1023/A:1020170320020

[21]: R. Peraldi, D. Monceau, B. Pieraggi, Correlations between growth kinetics and microstructure for scales formed by high-temperature oxidation of pure nickel, II. Growth Kinetics, Oxid. Metals 58 (2002) 275-295.

https://doi.org/10.1023/A:1020102604090

[22]: R. Haugsrud, On the high-temperature oxidation of nickel, Corrosion Science 45 (2003) 211-235.

https://doi.org/10.1016/S0010-938X(02)00085-9

[23]: D. Vrel, P. Langlois, E.M. Heian, N. Karnatak, S. Dubois, M.F. Beaufort, Reactions kinetics and phase segregation in the 3NiO + 2Al → 3Ni+ Al_2O_3 Thermite system, International Journal of High-Temperature Synthesis 12 (2004) 261-270.

[24]: D. Vrel, A. Hendaoui, P. Langlois, S. Dubois, V. Gauthier, B. Cochepin, SHS reactions in the NiO-Al system: influence of stoichiometry, International Journal of High-Temperature Synthesis 16 (2007) 62-69.

https://doi.org/10.3103/S1061386207020021

[25]: A. Atkinson, R.I. Taylor, P.D. Goode, Transport processes in the oxidation of Ni studied using tracers in growing NiO scales, Oxidation of Metals 13 (1979) 519-543.

https://doi.org/10.1007/BF00812776

[26]: N.N. Khoi, W.W. Smeltzer, J.D. Embury, Growth and structure of nickel oxide on nickel crystal faces, Journal of The Electrochemical Society 122 (1975) 11.

[27]: A. Atkinson, F.C.W. Pummery, C. Monty, Diffusion of ^{18}O tracer in NiO grain boundaries, Transport in Nonstoichiometric Compounds 129, 359–370, Plenum Press, New York 1985.

https://doi.org/10.1007/978-1-4613-2519-2_27

[28]: R.A. Rapp, The high temperature oxidation of metals forming cation-diffusing scales, Metallurgical Transactions A, 15 (1984) 765-782.

https://doi.org/10.1007/BF02644552

[29]: C.K. Kim, L.W. Hobbs, Microstructural evidence for short-circuit oxygen diffusion paths in the oxidation of a dilute Ni-Cr alloy, Oxidation of Metals 45 (1996) 247-265.

https://doi.org/10.1007/BF01046984

[30]: S.K. Verma, G.M. Raynaud, R.A. Rapp, Chemical metallurgy: a tribute to Carl Wagner, The Metallurgical Society of AIME 419–40, New-York 1981.

[31]: A. Brückman, R. Emmerich, S. Mrowec, Investigation of the high-temperature oxidation Fe-Cr alloys by means of the isotope ^{18}O, Oxidation of Metals 5 (1972) 137-147.

https://doi.org/10.1007/BF00610841

[32]: A. Brückman, The mechanism of transport of matter through the scales during oxidation of metals and alloys, Corrosion Science 7 (1967) 51-54.

https://doi.org/10.1016/S0010-938X(67)80069-6

[33]: S. Mrowec, On the mechanism of high-temperature oxidation of metals and alloys, Corrosion Science 7 (1967) 563-578.

https://doi.org/10.1016/0010-938X(67)80033-7

[34]: G.J. Yurek, H. Schmaltzried, Deviation from local thermodynamic equilibrium during interdiffusion of CoO–MgO and CoO–NiO, Berrichte Der Bunsengesellschaft Für Physikalische Chemie, 79(3) (1975) 255-262.

https://doi.org/10.1002/bbpc.19750790304

[35]: A. Atkinson, D.W. Smart, Transport of nickel and oxygen during the oxidation of nickel and dilute nickel/chromium alloy, Journal of The Electrochemical Society 135 (1988) 11.

https://doi.org/10.1149/1.2095454

[36]: J. Robertson, M.I. Manning, Criteria for formation of single layer, duplex, and breakaway scales on steels, Materials Science and Technology 4 (1988) 12.

https://doi.org/10.1179/mst.1988.4.12.1064

[37]: A.G. Evans, D. Rajdev, D.L. Douglass, The mechanical properties of nickel oxide and their relationship to the morphology of thick scales formed on nickel, Oxidation of Metals 4 (1972) 151-170.

https://doi.org/10.1007/BF00613090

[38]: P. Kofstad, On the formation of porosity and microchannels in growing scales, Oxidation of Metals 24 (1985) 265-276.

https://doi.org/10.1007/BF00657061

[39] A. Atkinson, R.I. Taylor, The diffusion of Ni in the bulk and along dislocations in NiO single crystals, Philosophical Magazine A 39 (1978) 581-595.

https://doi.org/10.1080/01418617908239293

[40] A. Atkinson, R.I. Taylor, The diffusion of ^{63}Ni along grain boundaries in nickel oxide, Philosophical Magazine A 46 (1980) 979-998.

https://doi.org/10.1080/01418618108239506